THE JOURNAL OF BIOLOGICAL CHEMISTRY VOL. 282, NO. 10, pp. 7405–7415, March 9, 2007

Human Follicular Lymphoma Cells Contain Oligomannose Glycans in the Antigen-binding Site of the B-cell Receptor*[S]

Received for publication, March 22, 2006, and in revised form, December 20, 2006 Published, JBC Papers in Press, December 29, 2006, DOI 10.1074/jbc.M602690200

Catherine M. Radcliffe[‡1], James N. Arnold[§2], David M. Suter[‡], Mark R. Wormald[‡], David J. Harvey[‡], Louise Royle[‡1], Yusuke Mimura[‡1], Yoshinobu Kimura[‡¶3], Robert B. Sim[§], Susana Inogès[‖], Mercedes Rodriguez-Calvillo[‖4], Natalia Zabalegui[‖], Ascensión López-Díaz de Cerio[‖], Kathleen N. Potter[5], C. Ian Mockridge[**5], Raymond A. Dwek[‡], Maurizio Bendandi[‖6], Pauline M. Rudd[‡7], and Freda K. Stevenson[**5]**

*From the [‡]Glycobiology Institute, [§]Medical Research Council Immunochemistry Unit, Department of Biochemistry, University of Oxford, South Parks Road, Oxford OX1 3QU, United Kingdom, the [¶]Department of Biofunctional Chemistry, Graduate School of Natural Science and Technology, Okayama University, Japan, the [‖]University Clinic of Navarre and Center for Applied Medical Research, 31008 Pamplona, Spain, and the **Molecular Immunology Group, Tenovus Laboratory, Cancer Sciences Division, Southampton University Hospitals Trust, Southampton SO16 6YD, United Kingdom*

Expression of surface immunoglobulin appears critical for the growth and survival of B-cell lymphomas. In follicular lymphoma, we found previously that the Ig variable (V) regions in the B-cell receptor express a strikingly high incidence of *N*-glycosylation sequons, N*X*(S/T). These potential glycosylation sites are introduced by somatic mutation and are lymphoma-specific, pointing to their involvement in tumor pathogenesis. Analysis of the V region sugars from lymphoma-derived IgG/IgM reveals that they are mostly oligomannose and, remarkably, are located in the antigen-binding site, possibly precluding conventional antigen binding. The Fc region contains complex glycans, confirming that the normal glycan processing pathway is intact. Binding studies indicate that the oligomannose glycans occupying the V regions are accessible to mannose-binding lectin. These findings suggest a potential contribution to lymphoma pathogenesis involving antigen-independent interaction of surface immunoglobulin of the B-cell receptor with mannose-binding molecules of innate immunity in the germinal center.

Expression of sIg[8] is critical for the survival of normal B-cells in the periphery, even in the absence of antigen (1), indicating that a stimulatory surface Ig-mediated signal, independent of antigen, is required (2). The majority of malignancies derived from mature human B-cells may also require such a signal, since sIg-negative tumors are rare. In FL, sIg retention is remarkable, since in most tumors, one Ig allele is compromised by the characteristic t(14;18) chromosomal translocation. (3, 4) In terms of pathogenesis, the translocation that up-regulates expression of the BCL-2 oncoprotein appears necessary, but not sufficient, for tumor development, since it can also occur in B-cells of healthy individuals (5). Other factors must be required for survival in the hostile germinal center (GC), where normal B-cells that fail to be selected by antigen usually die.

FL occurs in the GC of lymph nodes, where tumor cells maintain many features of normal GC B-cells. A nodular or nodular/diffuse growth pattern is characteristic, with conservation of the microenvironment of follicular dendritic cells and CD4+ T cells. In normal B-cells, the Ig V region genes undergo somatic mutation in the GC. B-cells expressing Ig sequences that can bind antigen are rescued from the default death pathway, allowing further differentiation and subsequent exit as plasma cells or memory B-cells (6, 7). Somatic mutation is also activated in FL cells, with evidence of ongoing mutational activity in tumor clones (8). Although Ig expression is retained, it has been difficult to envisage a role for multiple potential antigens in supporting the growth of neoplastic B-cells. Interestingly, we observed a striking difference in the B-cell receptor of lymphoma cells as compared with normal B-cells, which might provide an alternative stimulatory pathway. In normal B-cells, *N*-glycosylation is mainly confined to conserved sites in the Ig constant regions, although a few germ line encoded V regions do carry potential *N*-glycosylation sites. In FLIg, the number of potential sites increases dramatically during the somatic mutation process. By analyzing V_H sequences, we previously found that 55 of 70 (79%) cases of FL contained these sequons. Sites were also present in V_L (9). This high incidence has been confirmed in 24 of 24 cases (10). Since glycosylation sites do not

* Glycan analysis was supported by the Oxford Glycobiology Institute endowment, and MALDI was supported by Biotechnology and Biological Sciences Research Council funding. The costs of publication of this article were defrayed in part by the payment of page charges. This article must therefore be hereby marked "*advertisement*" in accordance with 18 U.S.C. Section 1734 solely to indicate this fact.

[S] The on-line version of this article (available at http://www.jbc.org) contains supplemental Tables S1–S3.

[1] Present address: Dublin-Oxford Glycobiology Laboratory, NIBRT, Conway Institute, University College, Dublin 4, Ireland.

[2] Supported by a Medical Research Council grant.

[3] Supported by Grant-in-Aid from the Ministry of Education, Science, and Culture of Japan.

[4] Supported by an FIS contract of the Spanish Ministry of Health.

[5] Supported by Tenovus, UK.

[6] A Scholar in Clinical Research of the Leukemia and Lymphoma Society.

[7] To whom correspondence should be addressed: Dublin-Oxford Glycobiology Laboratory, NIBRT, Conway Institute, University College Dublin, Belfield, Dublin 4, Ireland. Tel.: 353-1-7166728; Fax: 353-1-7166713; E-mail: pauline.rudd@nibrt.ie.

[8] The abbreviations used are: sIg, surface immunoglobulin; BL, Burkitt's lymphoma; CLL, chronic lymphocytic leukemia; CLR, C-type lectin receptor; FL, follicular lymphoma; GC, germinal center; GU, glucose unit(s); MALDI, matrix-assisted laser desorption ionization; TOF, time-of-flight; MBL, mannose-binding lectin; NIgG, normal human IgG; NIgM, normal human IgM; NP, normal phase; PNGase F, peptide *N*-glycanase F; V region, variable region; HC, heavy chain; LC, light chain; 2AB, 2-aminobenzamide; HPLC, high pressure liquid chromatography; FITC, fluorescein isothiocyanate.

accumulate significantly in somatically mutated normal B-cells, the positive selection of B-cells in FL that express B-cell receptor containing *N*-linked glycans suggested a potential role for the oligosaccharides in tumorigenesis.

Sites generated by somatic mutation are frequent and possibly mandatory in FL, but they also exist in other GC-associated lymphomas (11). The incidence of potential *N*-glycosylation sites in endemic Burkitt's lymphoma (BL) is high (82%), although sporadic BL and diffuse large cell lymphoma have lower levels, 43 and 41%, respectively (9), possibly reflecting the known heterogeneity of these tumors. In contrast to GC-associated B-cell malignancies, sites are found at insignificant levels in chronic lymphocytic leukemia (CLL) and multiple myeloma (9).

The process of *N*-linked glycosylation is initiated in the ER by the transfer of the dolichol phosphate oligosaccharide precursor, *N*-acetylglucosamine$_2$-mannose$_9$-glucose$_3$, to suitable asparagine residues in the glycosylation sequons of nascent proteins (12). Following the removal of glucose and mannose residues, the fully folded protein is transported to the Golgi, where enzymes further process the glycans to hybrid and complex-type. The exact processing of the glycans depends on factors such as the cell in which the glycoprotein is expressed and the three-dimensional structure of the protein around the glycosylation site (13, 14). When enzyme access is restricted, oligomannose sugars may not be fully processed.

We have now characterized the glycosylation of the Fab region of FLIgs that results from somatic mutation and probed the accessibility of the glycans to C-type lectins. We have analyzed V region-associated sugars in tumor-specific Ig derived from six cases of FL. We focused first on IgG-expressing cases, since there are no conserved sites in the IgG Fab constant regions, analyzing heavy chain (HC), light chain (LC), and Fab fragments. Interestingly, the Fab glycans are mostly unprocessed oligomannose. FLIgM HC, which has a conserved glycosylation site in the constant region at Asn^{171} occupied by complex glycans, was also analyzed and showed a significant increase in oligomannose sugars when compared with normal human serum IgM (NIgM) (15, 16).

Studies with MBL, a C-type lectin, with both immobilized FLIgG and sIg, which is part of the B-cell receptor, have revealed that the terminal mannose residues on the Fab glycans are accessible for binding. Molecular modeling based on amino acid substitution of the Fab region has been used to ascertain the location of *N*-linked glycosylation sites.

EXPERIMENTAL PROCEDURES

Idiotypic Ig Production and Identification of Tumor-derived Gene Sequences—Six patients with Stage IVA FL had surgical biopsy at first relapse following chemotherapy; five expressed sIgG, and one expressed sIgM. The control patient had IgG$^+$ CLL, which expressed IgG without a potential V region *N*-glycosylation site. Ig protein was generated from tumor cells isolated from blood by producing heterohybridomas with the K6H6/B5 cell line (ATCC: CRL1823) as previously described (17–19). Resulting hybridomas were screened by enzyme-linked immunosorbent assay for the production of Ig matching the isotype of the tumor. The identities of fusions and tumor were determined by comparing Ig V_H CDR3 sequences. Ig was purified from culture supernatants by affinity chromatography (IgG, Protein A (Amersham Biosciences); IgM, anti-IgM antibody columns). Protein purity was determined by SDS-PAGE electrophoresis and in each case was >95%. All Ig proteins were adjusted to a final concentration of 1 mg/ml. V_H and V_L gene sequences were determined as previously described (9).

N-linked Glycan Analysis—15 μg of five FLIgG samples (FL2, -4, -11, -31, and -32), one FLIgM (FL3), CLL1, normal human serum NIgG, and NIgM were run on 10% SDS-polyacrylamide gels (20, 21). HC and LC protein bands migrating with an apparent molecular mass of 53–58 and 24–30 kDa, respectively, for IgG and 75–90 and 29 kDa, respectively, for IgM were excised, cut into ~1 mm^3, frozen for ~2 h at −20 °C, and washed with alternating 1 ml of acetonitrile and 1 ml of 20 mM $NaHCO_3$ pH 7 (five washes, 30 min each). *N*-Linked glycans were released *in situ* with peptide-*N*-glycanase F (PNGase F; Roche Applied Science) (20). The extracted glycans were labeled with the fluorophore 2-aminobenzamide (2AB; Ludger Ltd., Oxford, UK) (22) and processed through normal phase (NP) HPLC (23). Neutral, monosialylated, and disialylated fractions were also collected from weak anion exchange HPLC and processed by NP-HPLC for further analysis and confirmation of NIgG, FL2, NIgM, and FL3 peak assignments.

Exoglycosidase digestions were carried out on 2AB-labeled glycan pools of *N*-linked glycans (23). Matrix-assisted laser desorption ionization time-of-flight (MALDI-TOF) mass spectra of unlabeled glycans were recorded as described previously (20).

Papain Digestion of IgG and Fab/Fc Separation—Digestion of IgG samples FL2, FL4, FL31, and NIgG (100 μg) was performed with 1 μg of papain (Sigma) in 250 μl of 0.1 M phosphate buffer containing 2 mM EDTA, 12 mM cysteine (pH 7) for 16 h. To test the completion of the digestion, aliquots (4 μl) were treated with 50 mM iodoacetamide at 4 °C for 30 min to inactivate papain, added to nonreducing SDS-sample buffer preheated to 100 °C, and heated at 100 °C for 3 min. The samples were analyzed by 8.5% SDS-PAGE. The papain digests were dialyzed against 0.01 M phosphate buffer (pH 8) overnight and applied to DEAE-cellulose (Whatman, Kent, UK) that was equilibrated with the same buffer and packed into microcolumns (~100–150-μl bed volume). Undigested IgG, Fab, and papain were eluted in flow-through fractions. Fc was eluted with phosphate-buffered saline, pH 7.4. The separation of Fab and Fc was confirmed by Western blotting using horseradish peroxidase-conjugated versions of goat anti-human κ chains, goat anti-human λ chains, and mouse anti-human IgG-Fc (Serotec). Glycans from Fab and Fc fractions were released from in-gel bands and analyzed.

PNGase F Digestion in Solution of FL2 Fab—8 μl of FL2 Fab were treated as above to inactivate the papain. 4 μl were incubated with PNGase F in solution for 36 h (24). The nonreduced sample was run on 8.5% SDS-PAGE together with an undigested aliquot.

MBL Purification and Binding Assay—Rabbit anti-MBL polyclonal antiserum was depleted of any anti-mannan antibodies on a mannan-agarose resin (catalog number M9917; Sigma) and then pre-equilibrated in phosphate-buffered saline,

TABLE 1

HC and LC gene segment usage and glycosylation sites

V(D)J gene segment usage was determined by aligning nucleotide sequences to germ line sequences in V-BASE using MacVector 6.5.3 sequence analysis software (Accelerys, Cambridge, UK). D gene segments could not be assigned due to insufficient homology.

Case	Ig	V_H	J_H	Percentage homology	V_L	J_L	Percentage homology	No. of sites/region	Sequence
				%			%		
FL2	IgG	3–21	6	90.2	1e	λ2/3	92.8	2/CDRH2	I**NGS**N
									S**NTS**S
								1/CDRH3	R**NCS**S
FL4	IgG	1–18	6	90.5	1b	λ2/3	94.0	1/CDRH3	R**NSS**S
FL11	IgG	3–72	6	86.4	1b	λ2/3	88.0	1/CDRH3	S**NCS**R
FL31	IgG	3–30	6	90.5	1b	λ1	97.0	1/CDRH3	K**NET**W
FL32	IgG	4–39	5	88.8	1e	λ2/3	95.2	1/CDRH2	G**NIS**S
								1/CDRL2	Y**NSS**N
FL3	IgM	4–59	2	85.6	2e	λ2/3	94.9	1/FRH1	L**NCT**V
								1/CDRH2	G**NIS**S
								1/FRL4	T**NLT**V
CLL1	IgG	3–73		93.3	A19		98.0		

0.5 mM EDTA (25). Purification was carried out as described previously (25, 26). MBL concentration was calculated using a standardized MBL detection enzyme-linked immunosorbent assay using mannan capture. Enzyme-linked immunosorbent assay plate (NUNC-Maxisorp) wells were coated with 100 μl of 10 μg/ml FLIgG. CLL1 was used as a negative control. The binding assay was performed as described previously (25).

Preparation of MBL Biotinylated with NHS-Biotin Bound to Streptavadin-FITC—Purified MBL (500 μg) in 10 mM Hepes, 1 M NaCl, 5 mM EDTA, pH 7.4, was made up to 20 mM $CaCl_2$ and concentrated on a 0.5 ml column of D-mannose immobilized on cross-linked 4% beaded agarose (catalog number M-6400; Sigma) which was washed with 50 mM Hepes, 150 mM NaCl, 10 mM $CaCl_2$, pH 7.5. MBL was eluted with 50 mM Hepes, 150 mM NaCl, 2.5 mM EDTA, pH 7.5, and 200-μl fractions were collected. The MBL-containing fractions (~400 μl) were made up to 500 μl with wash buffer and incubated on ice for 30 min with a 25-fold molar excess over MBL (molecular mass taken as 300 kDa) of biotin 3-sulfo-*N*-hydroxysuccinimide ester (Sigma), from 1 mg/ml stock freshly made up in wash buffer. The reaction was stopped by adding 100 μl of 1 M Tris, pH 7.8, and incubating on ice for 10 min. The material was run as before on 0.5 ml of mannose-agarose resin. Eluted MBL was cross-linked using 1.3 μl of streptavidin-FITC (1 mg/ml, 60 kDa) (Sigma) to 50 μg of biotinylated MBL (4-fold molar excess), allowing 2-h intervals at 4 °C in the dark between each streptavidin-FITC addition.

MBL Cell Binding Assay—A telomerase-immortalized human HK cell line, derived from a follicular dendritic cell, and the EBV-ve BL cell line L3055 were obtained from Dr. Y. S. Choi (Cellular Immunology, Ochsner Clinic Foundation, New Orleans, LA). L3055 cells that express surface IgMλ with a known *N*-glycosylation site (27) were grown on HK feeder cells as previously described (28). After overnight incubation of HK cells at 5×10^5/well (in 3 ml of Iscove's modified Dulbecco's medium with 10% fetal calf serum, 1 mM pyruvate, 2 mM glutamine, nonessential amino acids, 20 units/ml penicillin, and 20 μg/ml streptomycin, all from Invitrogen), 7×10^4 L3055 cells were added per well and harvested after 2–3 days of incubation. BL-2 is an EBV-ve BL cell line (gift from Dr. A. Rickinson, University of Birmingham Medical School, Birmingham, UK). It expresses surface IgMλ with no *N*-glycosylation sites (27). BL-2 cells were grown as previously described (27, 28).

For each assay, 1×10^6 cells (L3055 or BL-2) were pelleted in 5-ml fluorescence-activated cell sorting tubes (1500 rpm, 5 min, 4 °C). Cells were resuspended in 500 μl of either HBSS (Sigma) supplemented with 5 mM $CaCl_2$ or 5 mM EDTA to demonstrate Ca^{2+}-dependent binding. The cells were centrifuged as before and resuspended in 250 μl of appropriate buffer and incubated with 5 μg (20 μg/ml) of FITC-conjugated MBL or 5 μg of goat anti-human IgM (μ chain-specific) for 30 min on ice prior to analysis on a BD Biosciences FACSCalibur. The effect of apoptosis on MBL binding to L3055 cells was investigated by dual staining with MBL-FITC followed by Annexin V-PE (BD Biosciences) according to the manufacturer's protocol.

L3055 and BL-2 cells were labeled with mouse anti-human Igλ FITC (BD Biosciences) and analyzed by fluorescence-activated cell sorting to determine surface immunoglobulin expression. To mediate endocytosis of sIg, L3055 cells were incubated overnight at 37 °C with goat $F(ab')_2$ anti-IgM (μ chain-specific) (Southern Biotech) at 10 μg/ml. Loss of sIg was monitored by staining with anti-human Igλ FITC, and the cells were then tested for MBL binding.

Molecular Modeling—Molecular modeling was performed as described previously (25). Briefly, sequence alignment was performed using Align (29) on the equivalent domains of IgG (Swiss-Prot: P01857) together with appropriate amino acid substitutions. Crystal structures used as the basis of the modeling were obtained from the Protein Data Bank (30). The structure of FL2 was based on the crystal structure of murine N1G9 antibody (31). The models of FL3, FL4, and FL31 were based on the crystal structure of the Fab domain of the monoclonal antibody against HIV-1 GP41 (32). *N*-Glycans were generated using the data base of glycosidic linkage conformations and *in vacuo* (33, 34) energy minimization to relieve unfavorable steric interactions.

RESULTS

V Gene Analysis—Analysis of gene segment sequences encoding V regions of FL cases (Table 1) show that a range of V_H and V_L genes were used, all of which were somatically mutated. In all cases, potential *N*-glycosylation sites N*X*(S/T) were identified. All contained sites in V_H; FL32 (IgG^+) and FL3 (IgM^+) each had an additional site in V_L. The position of sites varied; FL2 contained two in CDRH2, at Asn^{52} and Asn^{52c}, and

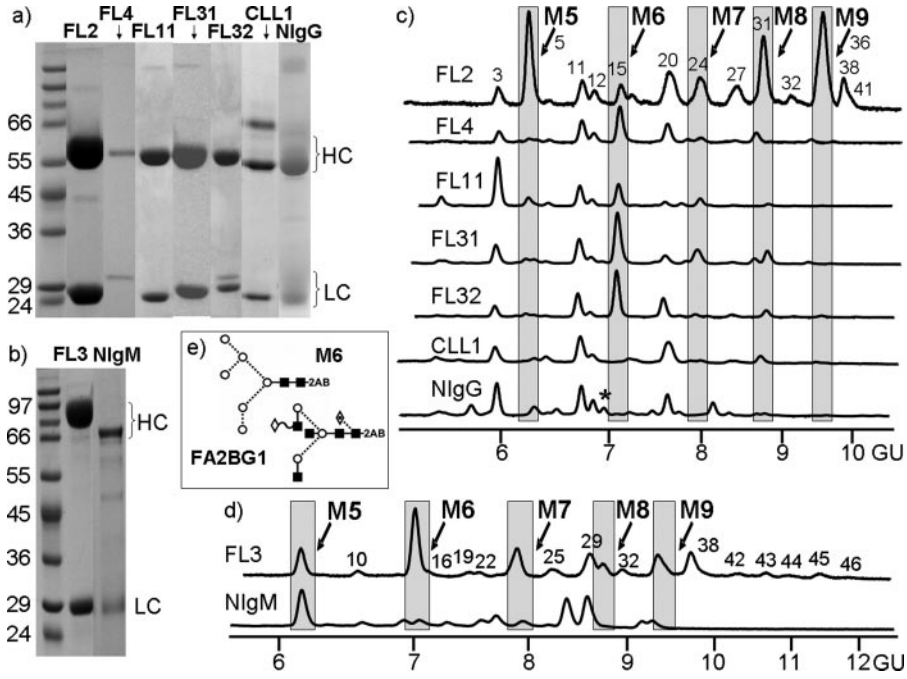

FIGURE 1. **Gels and NP-HPLC glycan profiles of FLIgs.** *a* and *b*, 10% SDS-polyacrylamide gels run under reducing conditions. An increase in molecular mass of FL HC bands is evident when compared with controls, which is indicative of glycosylation. *c*, profiles of FLIgG HC and two controls. Glycans contained in the two controls, CLL1 and NIgG, are evident in the FLIgG samples, interspersed with oligomannose, M5–M9. *d*, profiles of FLIgM (FL3) together with NIgM. Major peaks are named or numbered (Tables 2 and 3). *, peak containing bisected structure, FA2BG1, present in human IgG but not in mouse glycans. *e*, structural representations of M6 and FA2BG1. *Open circle*, mannose; *filled square*, GlcNAc; *open diamond*, galactose; *open diamond with dot*, fucose; *M*, mannose; *F*, α1–6 core fucose; *A*, antennary; *B*, bisected; *G*, galactose. Linkage is indicated by the angle linking adjacent residues. |, 1–2; /, 1–3; –, 1–4; \, 1–6; *dotted line*, α linkage; *solid line*, β linkage; ~, unknown linkage. The NP-HPLC system was calibrated using an external standard of hydrolyzed and 2AB-labeled glucose oligomers to provide a dextran ladder from which the retention times for the individual glycans were converted to GU. These were compared with the Glycobiology Institute data base of experimental values to obtain preliminary assignments for the glycans that were confirmed by digestions with arrays of exoglycosidases and mass spectrometry.

one in CDRH3 at Asn^{95}. In FL2, both CDRH2 sites resulted from codon insertions, with a Gly residue inserted between Asn and Ser and an Asn residue inserted prior to TS. The other four patient IgG samples each had a single site in V_H: FL4 at Asn^{95}, FL11 at Asn^{96}, FL31 at Asn^{95}, all in CDRH3, and FL32 at Asn^{50} in CDRH2. FL32 also had a potential site in V_L within CDRL2 at Asn^{50}. FL3 had two potential sites at Asn^{21} in framework region H1 and Asn^{50} in CDRH2 and a potential site in V_L within framework region L4 at Asn^{103}. The Ig derived from CLL1 as a hybridoma control had none.

N-linked Glycan Analysis—Ig secreted by tumor-derived heterohybridoma cells was run on 10% SDS-polyacrylamide gels under reducing conditions. Five patient-derived IgG samples and one IgM sample were analyzed together with three controls, CLL1, NIgG, and NIgM. The gel (Fig. 1*a*) shows that the HC of CLL1 and NIgG migrated with an apparent molecular mass of 55 kDa, whereas all of the patient samples were ~58 kDa, which is consistent with the glycosylation of the Fab region. Glycosylation was also indicated for FL3 HC, since it migrated with an apparent molecular mass of 90 kDa (Fig. 1*b*), whereas NIgM HC migrated at 75 kDa. The LC of FLIgG migrated between 24 and 30 kDa. The LC of both NIgM and FL3 had an apparent molecular mass of 29 kDa, suggesting a lack of glycosylation of the FL3 LC although it has a potential site.

Complete NP-HPLC glycan profiles were obtained for the 2AB-labeled HC glycans of all patient-derived samples and controls (Fig. 1, *c* and *d*). The system was calibrated using an external standard of hydrolyzed and 2AB-labeled glucose oligomers to create a standard curve. The retention times for the individual glycans were converted to glucose unit (GU) values using this curve. Preliminary peak assignments were made by comparing the GU values with the Oxford Glycobiology data base of experimental values, and the assignments were confirmed by exoglycosidase array digestions (23). These were carried out to remove the monosaccharides sequentially to elucidate the structures. Weak anion exchange HPLC data were used to facilitate the assignments of neutral and sialylated peaks of FL2 that coeluted (data not shown). All of the FLIgG samples contained the characteristic profile of complex glycans seen in NIgG (peaks 3, 11, 12, 20; Table 2 and supplemental Table S1), but there was unexpectedly also an oligomannose (M) series, M5–M9 (peaks 5, 15, 24, 31, and 36), with both types of glycan in varying proportions (Fig. 1, Table 2, and supplemental Table S1). The complex glycans were consistent with previous analyses of serum IgG Fc (35, 36), confirming that the normal glycan processing pathway was intact. CLL1 showed a characteristic IgG HC glycan NP-HPLC profile with 30% fucosylated (F; for assignment nomenclature, see Tables 2 and 3), agalactosylated, and monogalactosylated (G1) glycans with only 1% sialylation (S) but lacking glycans with bisecting (B) GlcNAc seen in human NIgG, marked with an *asterisk* in Fig. 1*c*. Structural representations of the biantennary (A2) glycan FA2BG1 and M6 are shown in Fig. 1*e*. A small percentage (~3%) of glycans terminating in α-galactose (Ga) was also found (Table 2 and supplemental Table S1). The presence of α-galactose (peaks 24, 27, 32, 35, 36, and 41) and the absence of bisected glycans in both control and patient samples indicated that the mouse glycosylation machinery is operative in all of these heterohybridomas, as shown elsewhere (37). The presence of M5–M9 suggested that these glycans were in positions inaccessible to mannosidase I and GlcNAc transferase I, the actions of which are required prior to processing to complex-type sugars. Together with the oligomannose-type, FL2 contained higher molecular mass glycans (*e.g.* biantennary structures, FA2G2S2 (7%), and FA2G2Ga1S2 (1%)) either absent in the other samples and controls or present in very small quantities (~1%) (Fig. 1*c*, Table 2, and supplemental Table S1). The production of more processed

TABLE 2
Peak assignments and percentage abundance of glycans of NIgG and FLIgGs

Peak number	Assignments[a]	NIgG[b]	CLL1[b]	FL2[b]	FL4[b]	FL11[b]	FL31[b]	FL32[b]
		%	%	%	%	%	%	%
1	A2	<1			2	7	3	1
2	A2B	<1						
3	FA2	17	14	3	8	35	11	8
5	M5			17	3	8	3	2
	FA1G1			1				
	FA2B	5						
6	A2G1(6)	<1	3	<1	2	1	3	1
8	A2G1(3)	<1	5	<1	3	2	1	<1
9	A2BG1(6)	<1						
11	FA2G1(6)	18	24	4	16	15	15	18
12	FA2G1(3)	9	6	2	7	4	4	3
13	FA2BG1(6)	5						
14	FA2BG1(3)	<1						
15	M6			3	25	16	32	35
	FM5A1			<1				
16	A2G2	1	5	2	2		2	
17	FA1G1S1			<1				
18	A2BG2	<1						
19	A2G1S1	<1	2	1	<1	<1	<1	<1
20	FA2G2	19	26	5	14	3	5	16
21	FA2BG2	4						
22	M5A1G1			1				
23	FA2G1S1	<1	1	1	2	2	1	1
24	FA3G2			6				
	M7				2	7	10	2
	FM5A1G1							
	A2G2Ga1							
25	A2G2S1	2		2	1		1	<1
27	FA2G2Ga1		3	3	2	1	1	3
28	FA3G3			1				
29	FA2G2S1	11	7	12	7	<1	2	2
30	FA2BG2S1	3						
31	M8			1	1	2	7	4
32	A2G2Ga1S1			2		<1		<1
34	A2G2S2	2	1	1	1		1	
35	FA2G2Ga1S1			4	1		1	
36	M9			20		<1	<1	2
	FA2G2Ga2							
38	FA2G2S2	2	<1	7	1		<1	
39	A2BG2S2	2						
41	FA2G2Ga1S2			1				<1

[a] A, antennary (followed by number of *N*-acetylglucosamine (GlcNAc) residues); A2, biantennary; B, bisect; F, α 1–6-linked core fucose; G, β -galactose; Ga, α -galactose; M, mannose; S, sialic acid; (3) or (6), linkage of G to GlcNAc on 3′ or 6′ arm of trimannosyl core, respectively.
[b] Percentage determined from NP-HPLC areas.

glycans is consistent with the more usual pattern of glycosylation that occurs in the ~10% of NIgG Fab where there is an *N*-glycosylation site due to somatic mutation that is fully accessible (38, 39).

FL32 has a potential *N*-glycosylation site on the LC, but no glycans were recovered. Molecular modeling showed that the site is on an exposed loop close to the V_H/V_L interface. Glycosylation could interfere with the assembly of the IgG, leading to the secretion of nonglycosylated isoforms only. None of the other IgG^+ LCs had potential glycosylation sites.

The glycans of NIgM (Table 3 and supplemental Table S2) were consistent with previous analyses (16). NIgM has five glycosylation sites on the HC (Asn^{171}, Asn^{332}, Asn^{395}, Asn^{402}, and Asn^{563}). Oligomannose glycans occupy conserved sites at Asn^{402} and Asn^{563} (15, 40). In this study, ~31% of the glycans from NIgM were oligomannose. This is consistent with 100% occupancy of Asn^{402}, which is homologous with Asn^{297} of IgG and is always fully occupied, and ~50% occupancy of Asn^{563}. It has been shown previously (16) that the oligomannose glycans in these conserved sites are not accessible for MBL binding. Two further NIgM samples had 28 and 30% oligomannose glycans (data not shown). FL3 (Fig. 1*d*, Table 3, and supplemental Table S2) showed an increase to ~49% oligomannose glycans, which is consistent with the occupancy of one of the two additional *N*-glycosylation sites in the Fab with oligomannose. The NP-HPLC profile shows that 9% of the glycans had a molecular mass higher than those of NIgM, including triantennary (A3) trisialylated (S3) structures (Table 3 and supplemental Table S2, peaks 42–46). The potential site on the LC contained oligomannose glycans, ~80% M6 and ~20% M5 (data not shown). Structural representations of all of the glycans from Tables 2 and 3 are shown in supplemental Table S3.

Jack Bean α-Mannosidase Digestions—The glycan pool of FL31 HC (Fig. 2*a*, Table 2, and supplemental Table S1) is representative of three other samples (FL4, -11, and -32). Jack bean α-mannosidase digestion of FL31 and FL2 glycans (Fig. 2, *b* and *d*) confirmed the presence of oligomannose glycans, and the profile remaining after removal of the mannose glycans was very similar to that of CLL1 (Fig. 1*c*). There are additional glycans (~3%) in the FL2 profile (Fig. 2*d*) that are hybrid structures (Peaks 17 and 22 and included in peaks 5, 15, and 24; Fig. 2*c*, Table 2, and supplemental Table S1) in which mannose residues on the 6′ arm of the trimannosyl core that were not processed by the glycosylation pathway enzymes have been digested. Structural representations of M5 and M7–M9 are included in Fig. 2. The presence of oligomannose glycans in FL3

TABLE 3
Peak assignments and percentage abundance of glycans of NIgM and FLIgM

Peak number	Assignment[a]	NIgM[b]	FL3[b]
		%	%
1	A2	<1	
2	A2B	<1	
3	FA2	<1	
4	A1G1		<1
5	M5	24	7
7	FA1G1	<1	<1
10	M4A1G1	2	2
13	FA2BG1	4	
15	M6	4	26
16	A2G2		<1
17	FA1G1S1(6)	2	<1
20	FA2G2	4	2
	A3G2	4	
	A2G1S1(6)	4	1
21	FA3G2/FA2BG2	7	
22	M5A1G1		<1
23	M4A1G1S1(6)		4
	FA2G1S1(6)		
24	M7	3	9
25	A2G2S1(6)	3	4
26	A2BG2S1	<1	
29	FA2G2S1(6)	17	9
30	FA2BG2S1	21	
31	M8		5
32	A2G2Ga1S1(6)		1
33	FA3G2S1(6)		<1
34	A2G2S2(6)		1
35	FA2G2Ga1S1(6)		7
36	M9		2
37	FA3G3S1(6)		<1
38	FA2G2S2(6,6)	4	9
	FA2G2S2(3,6)	4	9
40	FA2BG2S2(6,6)	5	
	FA2BG2S2(3,6)	5	
42	FA3G3Ga1S1(6)		2
	A3G3S2(6,6)		2
	FA3G3S2(3,6)		2
	FA3G3S2(6,6)		2
43	FA3G3S2(3,3)		2
	FA3G3Ga1S2(6,6)		2
44	FA3G3S3(3,3,6)		1
45	FA3G3S3(3,6,6)		3
46	FA3G3S3(6,6,6)		1

[a] A, antennary (followed by number of *N*-acetylglucosamine residues); A2, biantennary; B, bisect; F, α 1–6-linked core fucose; G, β -galactose; Ga, α -galactose; M, mannose; S, sialic acid; (3) or (6), α2–3- or α2–6-linked sialic acid.
[b] Percentage determined from NP-HPLC areas.

(Fig. 2*e*) was also confirmed. Again, there are additional structures from digested hybrid glycans (Fig. 2*f*). Details of GU values, peak areas, and mass spectrometry of both FLIgM and NIgM are shown in Table 3 and supplemental Table S2.

Papain Digestion of IgG—In order to confirm the location of the oligomannose glycans, the Fab and Fc regions were cleaved by papain digestion. The HC of NIgG was also digested by papain. Fractions containing Fab and Fc were confirmed by Western blotting (Fig. 3, *a*, *b*, *c*, and *d*). Fab and Fc fractions of NIgG, FL2, and FL4 were separated by DEAE. Separation of the corresponding fractions of FL31 was achieved by SDS-PAGE alone (Fig. 3*c*). FL2 Fab, which migrated as three bands (Fig. 3*d*), was digested by PNGase F in solution. The three bands collapsed into two, *x* and *y* (Fig. 3*e*). Glycan analysis of these bands showed that the protein in the major band *y* was not glycosylated, and the minor band *x* contained only M9 caused by incomplete digestion (data not shown). Variable occupancy of the three *N*-linked glycosylation sites was therefore confirmed.

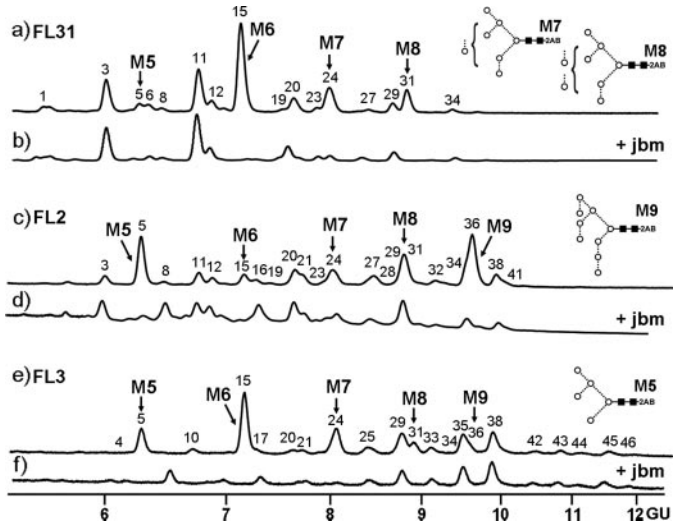

FIGURE 2. **NP-HPLC profiles of FLIg with jack bean α-mannosidase digestions.** FL31 (*a*), FL2 (*c*), and FL3 (*e*) are undigested glycan pools together with *b*, *d*, and *f*, which are jack bean α-mannosidase digestions. Oligomannose peaks are labeled. The removal of these peaks confirms the presence of oligomannose glycans and reveals the presence of complex glycans and profiles that correlate with normal controls. In the profiles of both FL2 and FL3, there is also evidence of hybrid structures in which mannose residues, on the 6′ arm of the trimannosyl core that were not processed by glycosylation pathway enzymes, have been digested. There are structural representations of M5 and M7–M9 (as described in the legend to Fig. 1).

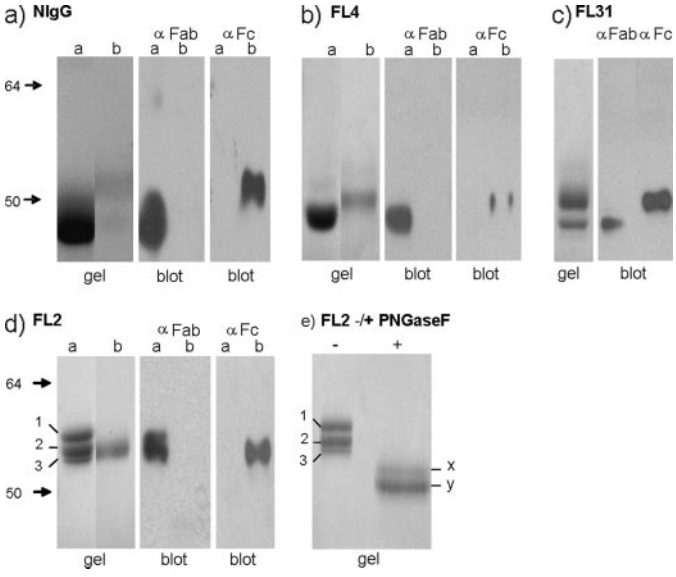

FIGURE 3. Glycoprotein staining and Western blot analysis of Fab and Fc fractions (*a*–*d*). 8.5% SDS-polyacrylamide gels and Western blots of Fab and Fc fractions of NIgG, FL4, FL31, and FL2. Fab and Fc fractions were obtained after DEAE chromatography of NIgG, FL4, and FL2 following papain digestion of FLIgG samples. *Lanes a*, flow-through fractions; *lanes b*, eluate. Separation of FL31 (*c*) was achieved by gel electrophoresis alone. FL4 and FL31 contained single bands of Fab, whereas FL2 (*d*) contained three, labeled *1*–*3*. *e*, FL2 Fab was treated with PNGase F in solution. The gel shows two bands. Following glycan analysis, *x* was shown to contain M9 due to incomplete deglycosylation, whereas *y* was completely deglycosylated.

Glycan Analysis of Fab and Fc Fractions—The Fab was shown to be glycosylated with oligomannose in three cases (Fig. 4), whereas the corresponding Fc contained only complex glycans. This, together with the position of the *N*-linked sequons, clearly locates the oligomannose glycans in the V region and also demonstrates the ability of the glycosyl transferases to

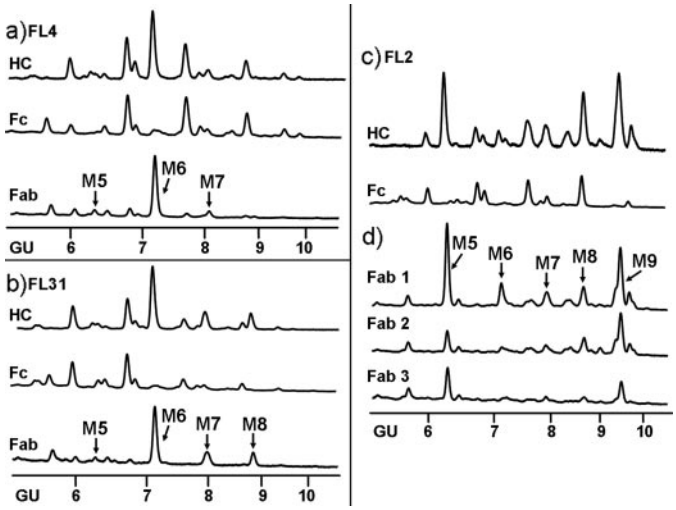

FIGURE 4. **NP-HPLC glycan profiles of HC, Fab, and Fc fractions.** FL4 (*a*) and FL31 (*b*) show HC glycosylation together with Fc and Fab, demonstrating the presence of oligomannose on the Fab fragments only. *c* and *d* show the chromatograms of FL2 glycans with the Fc without oligomannose plus three glycosylated Fab bands. The combination of complex and oligomannose glycans in Fab2 and -3 indicates that there may not have been complete separation of the two bands by SDS-PAGE.

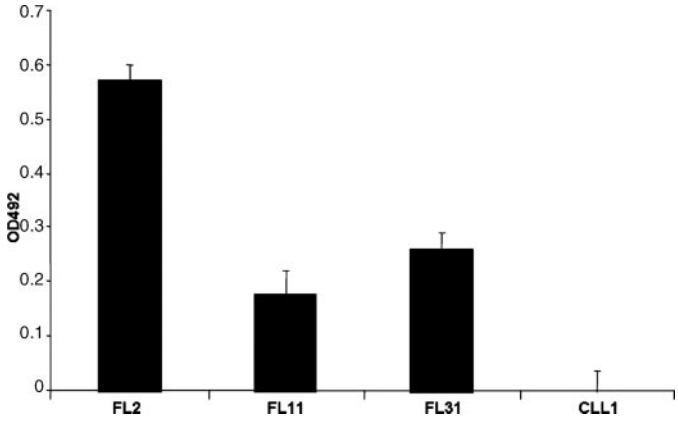

FIGURE 5. **MBL binding to three FLIgG samples, FL2, FL11, and FL31.** MBL binding to FLIgG immobilized on microtiter plates was assessed. Binding to FL2 is approximately twice that of the other two samples. FL2 has two *N*-linked glycosylation sites in the antigen-binding region; FL11 and FL31 each have a single *N*-linked glycosylation site. CLL1 is a negative control. The *bars* show the mean binding ± 1 S.D. Mannan was used as a positive control. The mean binding less the EDTA control was 3.783 ± 0.094 S.D. (data not shown).

process complex glycans in the Fc regions. Although FL4 and FL31 appeared to contain only oligomannose glycans (Fig. 4, *a* and *b*), the three bands of FL2 Fab contained both oligomannose and complex glycans (Fig. 4*d*). The high proportion (~69%) of oligomannose glycans from the fully occupied Fab1 indicates that mannosidase I and GlcNAc transferase I have restricted access to two of the sites. Half of the ~31% complex glycans consisted of triantennary and biantennary structures with the addition of α-galactose plus mono- and disialylation. This compares with no triantennary structures and 5% disialylation of the Fc, confirming that the third glycosylation site is more accessible than the Fc to the glycosylation pathway enzymes. The mixture of oligomannose and complex glycans on Fab2 and -3 bands, ~59 and ~71% oligomannose, respectively, indicates that there may not have been complete separation of the two bands by SDS-PAGE. The ~59% of oligomannose of Fab2 suggests that the two sites are occupied by one oligomannose and one complex/hybrid-type glycan (38/3%, respectively). About 10% of the Fab of NIgG HC contained complex structures, including glycans of molecular mass higher than those on the Fc, as has been shown previously (data not shown) (39). The two other papain-digested samples, FL4 and FL31, had ~73% (63% M6) and 88% (56% M6) oligomannose glycans, respectively, with a small percentage of complex glycans. With FL4, these could be from small quantities of Fc that were not completely retained by DEAE-cellulose chromatography. With FL31, complete separation was achieved by SDS-PAGE, indicating that ~10% of the glycans were processed to complex glycans. These data are consistent with one glycosylation site in the Fab region. Analysis of the Fc regions (Fig. 4, *a*–*c*) also revealed some differences between the samples. FL2 and FL4 have similar quantities of asialylated, agalactosylated (14%), and monogalactosylated (30%) structures, whereas FL31 contains 27 and 45% respectively. A reduction in galactosylation is known to be related to age and to some diseases, in particular rheumatoid arthritis and Crohn disease (41, 42). FL2 has 32% monosialylated structures with and without core fucosylation, whereas FL4 and FL31 have 21 and 11%, respectively. This demonstrates some differences in the activities of galactosyl and sialyl transferases of the individual tumor-derived heterohybridoma cell lines.

IgG Fab has *N*-glycosylation sites acquired only through somatic mutation, whereas IgM Fab has a conserved *N*-glycosylation site at Asn^{171}, occupied by complex glycans (43), in the C_H region as well as the possibility of sites acquired through somatic mutation. The glycan pool released from FLIgM Fab would therefore include glycans from both regions. The contribution from glycosylation resulting from somatic mutation in FLIgM was elucidated by comparing the percentage changes of the total glycan pool with those from NIgM.

MBL Binding Assay—MBL bound to all three FLIgGs tested, confirming that the terminal mannose residues were accessible to the lectin. Mannan and CLL1 were used as positive and negative binding controls, respectively. Protein concentrations for the Igs were normalized to CLL1 to account for MBL binding to any terminal GlcNAc present in the Fc (44). The graph in Fig. 5 shows that MBL binds most strongly to FL2, which has three glycosylation sites, two of which are occupied by oligomannose glycans. The binding is approximately twice that of the other two samples, which correlates with the single mannosylated site in the Fab of FL11 and FL31.

Binding of MBL to sIgM—To assess specific binding of MBL to cell surface Ig, two Burkitt's lymphoma cell lines were used. Motifs similar to those in FL have been found in these GC-associated B-cell tumors. FL cell lines were not used, since they are not as well characterized, and there would be no negative control. Two parallel Epstein-Barr virus-negative cell lines, each derived from sporadic BL and expressing comparable levels of sIgM, were analyzed (Fig. 6, *a* and *b*). In both cases, V_H4 gene segments were used to encode Ig V_H, but L3055 carries an *N*-linked glycosylation site in CDR2, whereas BL-2 has no motif (27). No sites were found in either of the V_L sequences. L3055

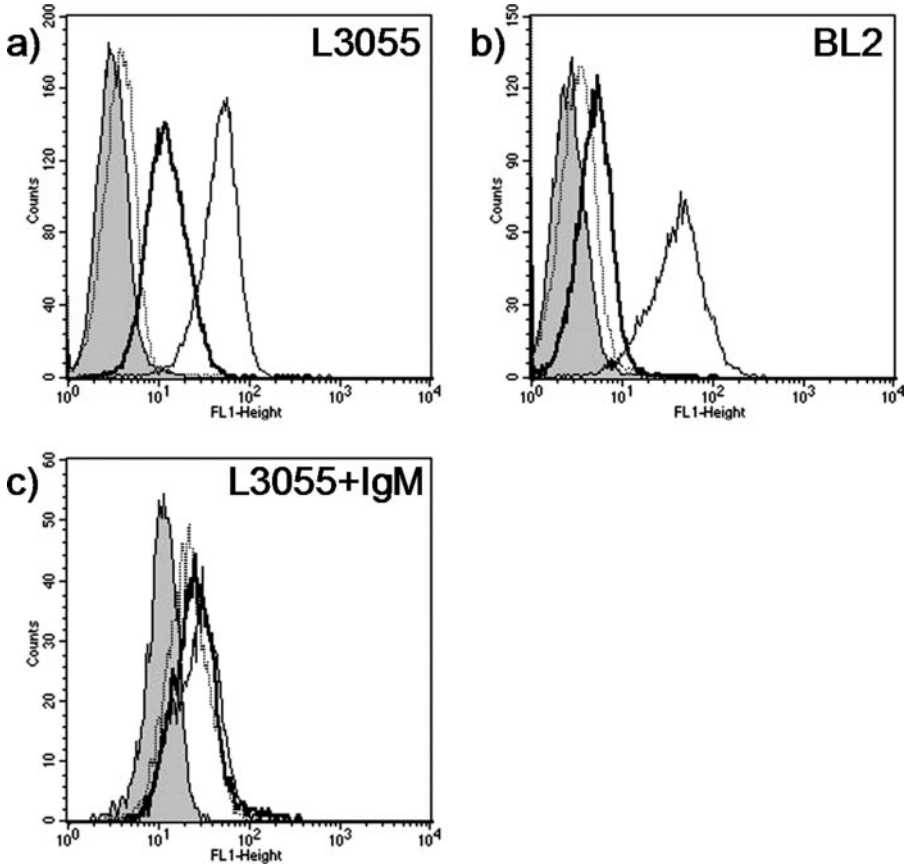

FIGURE 6. **Surface IgM expressed by L3055 cells binds to MBL.** L3055 cells (glycosylation site in V_H) (*a*) and control BL-2 cells (no glycosylation site in V_H or V_L) (*b*) expressed similar levels of sIg (*thin lines*). Each cell line was incubated with biotinylated MBL preconjugated with streptavidin-FITC in the presence or absence of Ca^{2+}. *a*, L3055 cells bound MBL (*thick line*), and binding was ablated in the absence of Ca^{2+} (*dotted gray line*). *b*, BL-2 cells bound very low levels of MBL (*thick line*), which was slightly reduced in the absence of Ca^{2+} (*dotted gray line*). *c*, L3055 cells were pretreated with goat $F(ab')_2$ anti-human IgM (μ chain-specific) overnight to remove sIgM by capping and endocytosis (*thin line*). In parallel, there was a reduction in binding of MBL (*thick line*) to that in the absence of Ca^{2+} (*dotted gray line*). The *filled histograms* represent unlabeled cells.

cells were able to bind to biotinylated MBL preconjugated with streptavidin-FITC, and this was ablated by removal of Ca^{2+} (Fig. 6*a*). In contrast, BL-2 cells showed only marginal binding of MBL, not significantly affected by removal of Ca^{2+} (Fig. 6*b*). This confirms that the oligomannose glycans in the conserved sites were not accessible for binding. Although viability was >90% and only viable cells were analyzed, L3055 cells tend to undergo apoptosis upon removal from HK cells (28). It was important, therefore, to assess any effects of early apoptosis on binding of MBL. Annexin V-positive and annexin V-negative L3055 cells showed similar binding to MBL, indicating no significant influence of apoptosis on binding (data not shown).

To correlate binding of MBL by L3055 cells with expression of sIgM, cells were treated with goat $F(ab')_2$ anti-human IgM (μ chain-specific) overnight in order to reduce surface expression by endocytosis. On gated live cells, there was a reduction in the expression of sIgM following endocytosis (Fig. 6*c*) as compared with the control (Fig. 6*a*). This was mirrored by a significant loss of ability to bind MBL, which became comparable with the low level of binding in the absence of Ca^{2+} (Fig. 6*c*). These data locate the binding of MBL to sIgM and strongly indicate that the glycosylation site in the Fab is critical for binding.

Molecular Modeling—Molecular modeling of the V regions of the Fabs of FL31 (Fig. 7) and FL4 (data not shown) has shown that the Fab glycosylation site (Asn^{95} in both cases) is in the antigen-binding groove. FL2 has two glycosylation sites (Asn^{52} and Asn^{95}) in the antigen-binding groove and one (Asn^{52c}) that is on an exposed loop (data not shown). The FL3 glycosylation site in the CDRH2 region (Asn^{50}) is also in the antigen-binding groove (data not shown). The model (Fig. 7) demonstrates that it is structurally feasible to have a typically folded Fab domain with glycans present at the site in the antigen-binding groove. Detailed examination of the model indicates that the diequatorial hydroxyl groups on C3 and C4 of terminal mannose residues are accessible, consistent with the experimental data that demonstrates the recognition of the glycans by MBL. However, access to the nonterminal glycan residues appears to be restricted by the location of the glycosylation sites in the antigen-binding groove and by the relatively long CDR loops, consistent with the observed lack of processing of these glycans by mannosidase I and GlcNAc transferase I. A $Man_6GlcNAc_2$ glycan was modeled on to the protein, since this was the most abundant glycan identifed in the FL31 Fab.

DISCUSSION

Tumor cells in the majority (~85%) of FL cases carry *N*-glycosylation sites in the CDRs (9, 10), and these cells are positively selected and functional (9). We have established the location and structures of the oligosaccharides attached to the V region of FLIg and their binding to the C-type lectin MBL and discuss their possible role in B-cell proliferation. Although most of the data in this paper are derived from protein secreted by heterohybridomas established from lymphoma cells, the evidence from the unmanipulated BL cell line points to a comparable expression of surface IgM with characteristics similar to those of FLIg.

V region glycans of sIgG and sIgM from FL tumor cells have been shown to be mostly oligomannose; in contrast, the Fc regions of the same molecules contain processed complex glycans, confirming that the normal glycan processing pathway is intact. In all of the FL cases, there is a high proportion of oligomannose, indicating an inaccessibility of these glycans to mannosidase I, which trims back the α1–2-linked mannose sugars, and to GlcNAc transferase I, which puts on the first GlcNAc

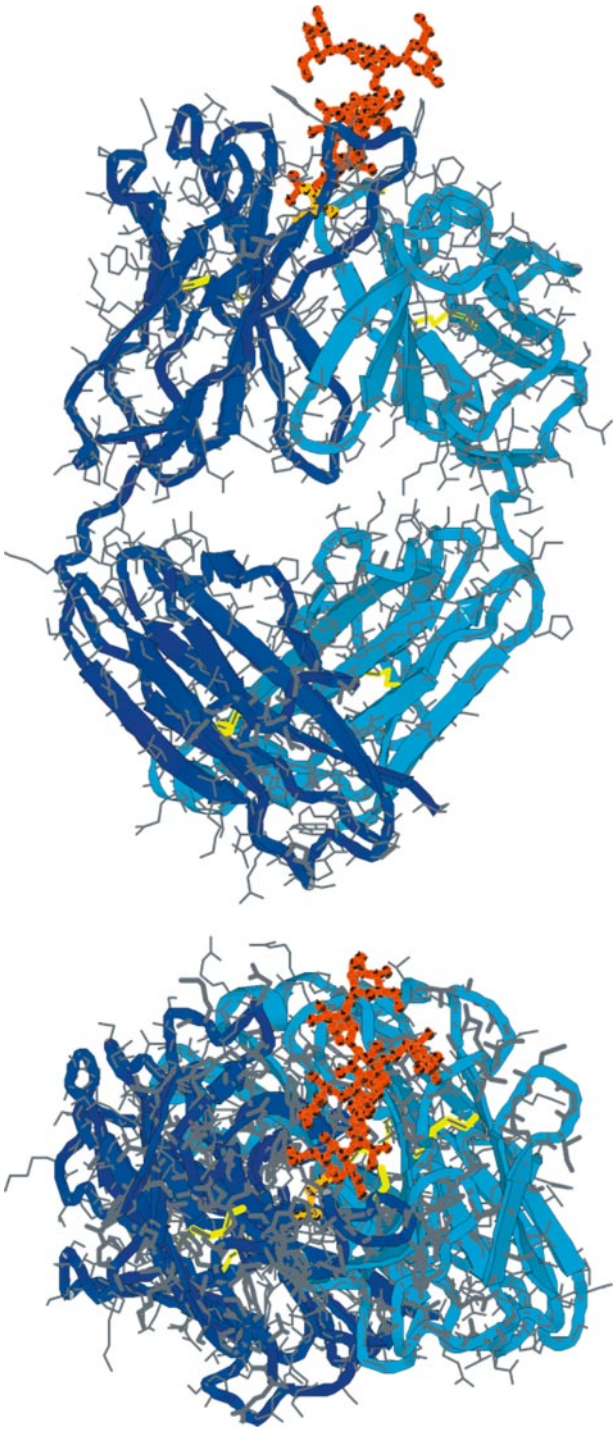

FIGURE 7. **Molecular models of FL31 Fab domains showing V_H glycosylation.** The molecule is shown in two orientations, side on (*above*) and looking down on the antigen-binding site (*below*). *Light blue*, LC; *dark blue*, HC; *yellow*, cysteines; *orange*, oligomannose glycans.

prior to the processing of complex structures. This allows the glycans to retain a composition not generally found at the cell surface. The Fab of both FL2 and FL3, which have three and two potential *N*-glycosylation sites, respectively, in the V regions, contained complex glycans in addition to the oligomannose, suggesting that sites are differentially glycosylated according to location. It is generally accepted that more exposed sites contain more highly processed glycans; however, amino acid sequence is also important, and the local three-dimensional protein structure is a major factor in regulating the degree of processing. For example, a study of the glycosylation of the influenza A virus hemagglutinin (45) showed that the glycan processing is site-specific and that one site that is buried in the hemagglutinin trimer contained only oligomannose glycans. The investigation of Thy-1 of rat brain and thymus (13) demonstrated that there is both tissue- and site-specific glycosylation and that the processing of oligosaccharides at one site is influenced by the glycosylation at other sites. A restriction in the processing of complex sugars was observed previously in the V regions of an artificially generated antibody expressed by a mouse hybridoma. The natural antibody had an NYT motif introduced at Asn^{58} in CDR2 of V_H following somatic mutation at position 60 (Asn to Thr). This site was glycosylated with complex sugars. However, site-directed mutagenesis of Lys^{62} to Thr resulted in the introduction of a new glycosylation site at Asn^{60}, which contained oligomannose glycans although the site was on the exposed loop of CDR2 (46, 47).

Molecular modeling of the Fab of FLIgG and FLIgM has revealed that, surprisingly, one or more glycosylation sites are located within the antigen-binding region, which would be expected to restrict the access of the processing enzymes. Glycan analysis has shown that the proportion of oligomannose glycans in the HC is consistent with complete occupancy of the antigen-binding regions in most cases. Where there is more than one potential glycosylation site in the V region, these occur both in the antigen-binding region and in more exposed positions. In FL2, when all the three potential sites are glycosylated, the proportions of oligomannose and complex glycans are consistent with two of the sites being occupied by oligomannose glycans and the third site by complex glycans.

The GC is a site where antigen-stimulated B-cells are selected or die, the decision being based mainly on the strength of antigen binding (48). Since sIg-negative tumors are rare, tumors located in the GC may retain a requirement for the engagement of sIg. FLIg bound to MBL, demonstrating the exposure of diequatorial hydroxyl groups at C3 and C4 on the terminal mannose (49) and indicating that C-type lectin receptors (CLR) could be involved in FL. Indeed, MBL is present on the surface of immature dendritic cells (DCs) (50). Other cell surface candidates for binding the oligosaccharides include mannose receptor, a CLR expressed on macrophages, DCs, and endothelium, and also endo 180, DEC-205, and DC-SIGN (51–53). CLRs are highly expressed on immature DCs, and DC-SIGN is expressed by DCs in lymphoid tissue and lymph nodes. A DC subset has been found that localizes within B-cell follicles (54). Interactions between the BL cell line L3055, which has sugars located in the CDR, and a follicular DC line have been shown to lead to the proliferation of L3055 cells (28). The normal function of the receptors of the innate immune system is to bind to pathogens, but they can also bind endogenous and self-ligands (53), suggesting a mechanism for the interaction of the oligomannose glycans with cell surface lectins that provides a substitute for antigen clustering.

The survival of patients with FL correlates with genes expressed by nonmalignant immune GC cells that infiltrate the tumor. Environmental signals from the GC cells, which

include follicular dendritic cells and macrophages, appear to promote survival or proliferation of malignant cells (55). It cannot be ruled out that the infiltrating cells may also interact with the oligomannose glycans on the surface of FL B-cells. It is also possible that the new glycosylation sites may alter local folding and domain structure, such that new peptide epitopes may become accessible and contribute to antigen-independent survival of FL B-cells.

The role of the oligomannose glycans is likely to be important in the early stage of tumor growth and is an example of the processes by which tumor cells adapt to and exploit hostile environments. At later stages, further chromosomal transformations would be expected to allow wider dissemination of tumor cells (8). In terms of therapy, the targeting of small molecules or antibodies to block the putative CLR interaction may be effective at the early stage of disease. It is possible that the highly effective treatment of lymphoma with anti-idiotypic antibody directed at sIg could be acting in this way (17, 56, 57). The unexpected finding that oligomannose sugars are covalently bound within the antigen-binding region of FLIgs opens up the possibility of novel therapeutic approaches to GC-associated lymphomas.

Acknowledgments—We thank Dr. Luisa Martinez-Pomares for helpful discussions and Dr. D. A. Mitchell for assistance with the biotinylation of MBL.

REFERENCES

1. Lam, K. P., Kuhn, R., and Rajewsky, K. (1997) *Cell* **90,** 1073–1083
2. Smith, S. H., and Reth, M. (2004) *Mol. Cell* **14,** 696–697
3. Tsujimoto, Y., Cossman, J., Jaffe, E., and Croce, C. M. (1985) *Science* **228,** 1440–1443
4. Yunis, J. J., Frizzera, G., Oken, M. M., McKenna, J., Theologides, A., and Arnesen, M. (1987) *N. Engl. J. Med.* **316,** 79–84
5. Limpens, J., Stad, R., Vos, C., de Vlaam, C., de Jong, D., van Ommen, G. J., Schuuring, E., and Kluin, P. M. (1995) *Blood* **85,** 2528–2536
6. Liu, Y. J., and Arpin, C. (1997) *Immunol. Rev.* **156,** 111–126
7. Manser, T. (2004) *J. Immunol.* **172,** 3369–3375
8. Zelenetz, A. D., Chen, T. T., and Levy, R. (1992) *J. Exp. Med.* **176,** 1137–1148
9. Zhu, D., McCarthy, H., Ottensmeier, C. H., Johnson, P., Hamblin, T. J., and Stevenson, F. K. (2002) *Blood* **99,** 2562–2568
10. Zabalegui, N., de Cerio, A. L., Inoges, S., Rodriguez-Calvillo, M., Perez-Calvo, J., Hernandez, M., Garcia-Foncillas, J., Martin-Algarra, S., Rocha, E., and Bendandi, M. (2004) *Haematologica* **89,** 541–546
11. Zhu, D., Ottensmeier, C. H., Du, M. Q., McCarthy, H., and Stevenson, F. K. (2003) *Br. J. Haematol.* **120,** 217–222
12. Dwek, R. A. (1996) *Chem. Rev.* **96,** 683–720
13. Parekh, R. B., Tse, A. G., Dwek, R. A., Williams, A. F., and Rademacher, T. W. (1987) *EMBO J.* **6,** 1233–1244
14. Rudd, P. M., and Dwek, R. A. (1997) *Crit. Rev. Biochem. Mol. Biol.* **32,** 1–100
15. Wormald, M. R., Wooten, E. W., Bazzo, R., Edge, C. J., Feinstein, A., Rademacher, T. W., and Dwek, R. A. (1991) *Eur. J. Biochem.* **198,** 131–139
16. Arnold, J. N., Wormald, M. R., Suter, D. M., Radcliffe, C. M., Harvey, D. J., Dwek, R. A., Rudd, P. M., and Sim, R. B. (2005) *J. Biol. Chem.* **280,** 29080–29087
17. Kwak, L. W., Campbell, M. J., Czerwinski, D. K., Hart, S., Miller, R. A., and Levy, R. (1992) *N. Engl. J. Med.* **327,** 1209–1215
18. Inoges, S., Rodriguez-Calvillo, M., Lopez-Diaz de Cerio, A., Zabalegui, N., Perez-Calvo, J., Panizo, C., Hernandez, M., Cuesta, B., Rocha, E., and Bendandi, M. (2003) *Haematologica* **88,** 1438–1440
19. Rodriguez-Calvillo, M., Inoges, S., Lopez-Diaz de Cerio, A., Zabalegui, N., Villanueva, H., and Bendandi, M. (2004) *Crit. Rev. Oncol. Hematol* **52,** 1–7
20. Radcliffe, C. M., Diedrich, G., Harvey, D. J., Dwek, R. A., Cresswell, P., and Rudd, P. M. (2002) *J. Biol. Chem.* **277,** 46415–46423
21. Kuster, B., Wheeler, S. F., Hunter, A. P., Dwek, R. A., and Harvey, D. J. (1997) *Anal. Biochem.* **250,** 82–101
22. Bigge, J. C., Patel, T. P., Bruce, J. A., Goulding, P. N., Charles, S. M., and Parekh, R. B. (1995) *Anal. Biochem.* **230,** 229–238
23. Guile, G. R., Rudd, P. M., Wing, D. R., Prime, S. B., and Dwek, R. A. (1996) *Anal. Biochem.* **240,** 210–226
24. Goodarzi, M. T., and Turner, G. A. (1998) *Glycoconj. J.* **15,** 469–475
25. Arnold, J. N., Radcliffe, C. M., Wormald, M. R., Royle, L., Harvey, D. J., Crispin, M., Dwek, R. A., Sim, R. B., and Rudd, P. M. (2004) *J. Immunol.* **173,** 6831–6840
26. Tan, S. M., Chung, M. C., Kon, O. L., Thiel, S., Lee, S. H., and Lu, J. (1996) *Biochem. J.* **319,** 329–332
27. Chapman, C. J., Zhou, J. X., Gregory, C., Rickinson, A. B., and Stevenson, F. K. (1996) *Blood* **88,** 3562–3568
28. Choe, J., Li, L., Zhang, X., Gregory, C. D., and Choi, Y. S. (2000) *J. Immunol.* **164,** 56–63
29. Pearson, W. R., Wood, T., Zhang, Z., and Miller, W. (1997) *Genomics* **46,** 24–36
30. Berman, H. M., Westbrook, J., Feng, Z., Gilliland, G., Bhat, T. N., Weissig, H., Shindyalov, I. N., and Bourne, P. E. (2000) *Nucleic Acids Res.* **28,** 235–242
31. Mizutani, R., Miura, K., Nakayama, T., Shimada, I., Arata, Y., and Satow, Y. (1995) *J. Mol. Biol.* **254,** 208–222
32. He, X. M., Ruker, F., Casale, E., and Carter, D. C. (1992) *Proc. Natl. Acad. Sci. U. S. A.* **89,** 7154–7158
33. Petrescu, A. J., Petrescu, S. M., Dwek, R. A., and Wormald, M. R. (1999) *Glycobiology* **9,** 343–352
34. Wormald, M. R., Petrescu, A. J., Pao, Y. L., Glithero, A., Elliott, T., and Dwek, R. A. (2002) *Chem. Rev.* **102,** 371–386
35. Parekh, R. B., Dwek, R. A., Sutton, B. J., Fernandes, D. L., Leung, A., Stanworth, D., Rademacher, T. W., Mizuochi, T., Taniguchi, T., Matsuta, K., Takeuchi, F., Nagano, Y., Miyamoto, T., and Kobata, A. (1985) *Nature* **316,** 452–457
36. Wormald, M. R., Rudd, P. M., Harvey, D. J., Chang, S. C., Scragg, I. G., and Dwek, R. A. (1997) *Biochemistry* **36,** 1370–1380
37. Tandai, M., Endo, T., Sasaki, S., Masuho, Y., Kochibe, N., and Kobata, A. (1991) *Arch. Biochem. Biophys.* **291,** 339–348
38. Kabat E. A., Wu, T. T., Perry, H. H., Gottesman, K. S., and Foeller, C. (1991) *Sequences of Proteins of Immunological Interest*, 5th Ed., National Institutes of Health, Washington, D. C.
39. Chang, S.-C. (1993) *Altered Glycosylation In Immunoglobulin G and Its Fragments in Rheumatoid Arthritis.* Ph.D. thesis in Biochemistry, University of Oxford
40. Chapman, A., and Kornfeld, R. (1979) *J. Biol. Chem.* **254,** 824–828
41. Parekh, R. B., Roitt, I. M., Isenberg, D. A., Dwek, R. A., Ansell, B. M., and Rademacher, T. W. (1988) *Lancet* **1,** 966–969
42. Parekh, R., Roitt, I., Isenberg, D., Dwek, R., and Rademacher, T. (1988) *J. Exp. Med.* **167,** 1731–1736
43. Fukuta, K., Abe, R., Yokomatsu, T., Kono, N., Nagatomi, Y., Asanagi, M., Shimazaki, Y., and Makino, T. (2000) *Arch. Biochem. Biophys.* **378,** 142–150
44. Malhotra, R., Wormald, M. R., Rudd, P. M., Fischer, P. B., Dwek, R. A., and Sim, R. B. (1995) *Nat. Med.* **1,** 237–243
45. Mir-Shekari, S. Y., Ashford, D. A., Harvey, D. J., Dwek, R. A., and Schulze, I. T. (1997) *J. Biol. Chem.* **272,** 4027–4036
46. Endo, T., Wright, A., Morrison, S. L., and Kobata, A. (1995) *Mol. Immunol.* **32,** 931–940
47. Gala, F. A., and Morrison, S. L. (2004) *J. Immunol.* **172,** 5489–5494
48. Wang, L. D., and Clark, M. R. (2003) *Immunology* **110,** 411–420
49. Weis, W. I., Taylor, M. E., and Drickamer, K. (1998) *Immunol. Rev.* **163,** 19–34
50. Downing, I., Koch, C., and Kilpatrick, D. C. (2003) *Immunology* **109,** 360–364

51. Cambi, A., and Figdor, C. G. (2003) *Curr. Opin. Cell Biol.* **15,** 539–546
52. Geijtenbeek, T. B., van Vliet, S. J., Engering, A., 't Hart, B. A., and van Kooyk, Y. (2004) *Annu. Rev. Immunol.* **22,** 33–54
53. McGreal, E. P., Martinez-Pomares, L., and Gordon, S. (2004) *Mol. Immunol.* **41,** 1109–1121
54. Berney, C., Herren, S., Power, C. A., Gordon, S., Martinez-Pomares, L., and Kosco-Vilbois, M. H. (1999) *J. Exp. Med.* **190,** 851–860
55. Dave, S. S., Wright, G., Tan, B., Rosenwald, A., Gascoyne, R. D., Chan, W. C., Fisher, R. I., Braziel, R. M., Rimsza, L. M., Grogan, T. M., Miller, T. P., LeBlanc, M., Greiner, T. C., Weisenburger, D. D., Lynch, J. C., Vose, J., Armitage, J. O., Smeland, E. B., Kvaloy, S., Holte, H., Delabie, J., Connors, J. M., Lansdorp, P. M., Ouyang, Q., Lister, T. A., Davies, A. J., Norton, A. J., Muller-Hermelink, H. K., Ott, G., Campo, E., Montserrat, E., Wilson, W. H., Jaffe, E. S., Simon, R., Yang, L., Powell, J., Zhao, H., Goldschmidt, N., Chiorazzi, M., and Staudt, L. M. (2004) *N. Engl. J. Med.* **351,** 2159–2169
56. Bendandi, M., Gocke, C. D., Kobrin, C. B., Benko, F. A., Sternas, L. A., Pennington, R., Watson, T. M., Reynolds, C. W., Gause, B. L., Duffey, P. L., Jaffe, E. S., Creekmore, S. P., Longo, D. L., and Kwak, L. W. (1999) *Nat. Med.* **5,** 1171–1177
57. Timmerman, J. M., Czerwinski, D. K., Davis, T. A., Hsu, F. J., Benike, C., Hao, Z. M., Taidi, B., Rajapaksa, R., Caspar, C. B., Okada, C. Y., van Beckhoven, A., Liles, T. M., Engleman, E. G., and Levy, R. (2002) *Blood* **99,** 1517–1526